

THE X-RAY BACKGROUND

A. J. Barger^{1,2,3}

RESUMEN

Hemos obtenido magnitudes B , V , R , I , y z' para las 370 fuentes puntuales de radio en la observación de aproximadamente 1 Ms del campo norte profundo del *Chandra* (CDF-N), magnitudes HK' para 276 fuentes, y corrimientos al rojo espectroscópicos para 182 fuentes. La distribución de z muestra indicios de estructuras en $z = 0.843$ y $z = 1.0175$ (también detectadas en sondeos ópticos) que podrían explicar en parte la variación observada entre campos contiguos en los recuentos de fuentes de rayos X. Las contribuciones al flujo separadas en celdas unitarias de z muestran que las fuentes con $z < 1$ espectroscópicamente identificadas contribuyen ya con cerca de un tercio del flujo total tanto en la banda dura como en la suave. Ello implica que se ha dado acreción en grande hacia agujeros negros supermasivos desde que el Universo tenía la mitad de su edad actual. A partir de los cocientes de los recuentos en rayos X encontramos que los espectros en rayos X quedan bien descritos por absorción con una ley de potencias con $\Gamma = 1.8$ (intrínseca) y con valores de N_H entre 10^{21} cm^{-2} y $5 \times 10^{23} \text{ cm}^{-2}$. Estimamos que las fuentes *Chandra* que producen el 87% del fondo de rayos X *HEAO-A* (XRB) a 3 keV producen el 57% a 20 keV, siempre y cuando la forma del espectro de estas fuentes a altas energías continúe siendo una ley de potencias con $\Gamma = 1.8$. Sin embargo, si se normalizan las contribuciones del *Chandra* al XRB del *BeppoSAX* a 3 keV, la forma concuerda bien con el XRB observado en ambas energías. Así, el que sea necesario postular una población considerable de fuentes gruesas en Compton para resolver completamente el XRB por arriba de 10 keV depende críticamente de la manera como se ligen las mediciones -actualmente discrepantes- del XRB para energías entre 1 – 10 keV con el XRB a energías mayores.

ABSTRACT

We obtained B , V , R , I , and z' magnitudes for the 370 X-ray point sources in the ≈ 1 Ms observation of the *Chandra* Deep Field North (CDF-N), HK' magnitudes for 276, and spectroscopic redshifts for 182. The redshift distribution shows indications of structures at $z = 0.843$ and $z = 1.0175$ (also detected in optical surveys) which could account for a part of the field-to-field variation seen in the X-ray number counts. The flux contributions separated into unit bins of redshift show that the $z < 1$ spectroscopically identified sources already contribute about one-third of the total flux in both the hard and soft bands. Thus, major accretion onto supermassive black holes has occurred since the Universe was half its present age. We find from ratios of the X-ray counts that the X-ray spectra are well-described by absorption of an intrinsic $\Gamma = 1.8$ power-law, with N_H values ranging from about 10^{21} cm^{-2} to $5 \times 10^{23} \text{ cm}^{-2}$. We estimate that the *Chandra* sources which produce 87% of the *HEAO-A* X-ray background (XRB) at 3 keV produce 57% at 20 keV, provided that at high energies the spectral shape of the sources continues to be well-described by a $\Gamma = 1.8$ power-law. However, when the *Chandra* contributions are normalized to the *BeppoSAX* XRB at 3 keV, the shape matches fairly well the observed XRB at both energies. Thus, whether a substantial population of as-yet undetected Compton-thick sources is required to completely resolve the XRB above 10 keV depends critically on how the currently discrepant XRB measurements in the 1 – 10 keV energy range tie together with the higher energy XRB.

Key Words: COSMOLOGY: OBSERVATIONS — GALAXIES: ACTIVE — GALAXIES: DISTANCES AND REDSHIFTS — GALAXIES: EVOLUTION

1. INTRODUCTION

The extragalactic background light (EBL) represents the accumulated energy production over the lifetime of the Universe, modulated only by the expansion losses. With the exception of the cosmic microwave background radiation, the EBL is believed to be produced by star formation and by accretion onto the supermassive black holes that power active

galactic nuclei. The key to mapping the universal history of the formation of stars and supermassive black holes is to trace the origin of the light. Once all the EBL has been accounted for, we will have a complete census of galaxies and supermassive black holes in the Universe.

Active galactic nuclei (AGN) dominate the X-ray background (XRB), star forming galaxies dominate the optical EBL, and obscured star forming galaxies and AGN dominate the far-infrared (FIR)/submillimeter EBL. *COBE* found

¹Department of Astronomy, U. Wisconsin, USA.

²Department of Physics and Astronomy, U. Hawaii, USA.

³Institute for Astronomy, U. Hawaii, USA.

that the total reradiated emission appearing in the FIR/submillimeter is comparable to the entire optical Universe.

X-ray surveys most directly trace accretion onto supermassive black holes and hence provide our best window on black hole evolution. Much of the accretion power of the Universe may be absorbed by substantial neutral hydrogen column densities (e.g., Fabian & Iwasawa 1999); thus, to construct a complete census of supermassive black holes to the earliest epoch, we need to be able to detect sources which are heavily obscured from soft X-ray energies to the near-infrared (NIR).

A fundamental goal of the *Chandra X-ray Observatory* was to resolve the hard (2–8 keV) XRB into discrete sources. At these energies the photons can penetrate all but the highest column densities of gas and dust, so many obscured AGN can now be detected. The two ≈ 1 Ms exposures of the *Chandra* Deep Field North (CDF-N; Brandt et al. 2001; the CDF-N exposure has recently been extended to a second megasecond) and the *Chandra* Deep Field South (CDF-S; Giacconi et al. 2002) resolved > 80 –90% of the 2–8 keV XRB into discrete sources (Campana et al. 2001; Cowie et al. 2002; Rosati et al. 2002), where the largest uncertainty is the XRB measurement itself. The field-to-field difference in the contribution to the XRB from the X-ray sources in the CDF-N and CDF-S is 40%; this is substantially above the Poisson noise expected from the number of sources, suggesting clustering.

2. OPTICAL PROPERTIES

We obtained multiwavelength data of the X-ray sources in the CDF-N to understand the nature and evolution of the sources creating the XRB. We have Suprime-Cam (Miyazaki et al. 1998) on Subaru imaging data of the 370 X-ray point sources in the CDF-N catalog of Brandt et al. (2001), as well as LRIS (Oke et al. 1995) on Keck and HYDRA (Barden et al. 1994) on WIYN spectroscopy of 182. (We obtained 175 of the spectra, while the remaining seven redshifts are from the compilation of Cohen et al. 2000.) We restricted our analysis to a $10'$ radius (294 arcmin^2) region, since beyond that the X-ray point spread function degrades rapidly. This sample contains 330 X-ray sources (10 are stars).

Most sources with $R \leq 24$ can be spectroscopically identified, while only a few can be identified at fainter optical magnitudes. The latter sources may either lie at $z = 1.5 - 3$ (based on the colors; Crawford et al. 2001; Barger et al. 2001a; Cowie et al. 2001) or at $z > 5$, if they are low luminosity quasars. (Cold dark matter models can allow a large number

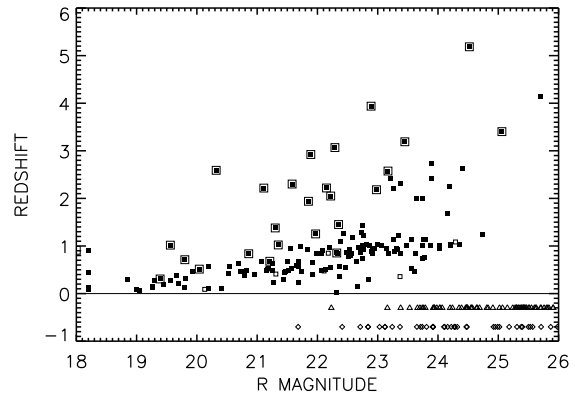


Fig. 1. Redshift versus R for the X-ray sources, excluding stars, within a $10'$ radius of the approximate X-ray image center. Saturated objects are plotted at $R = 18.2$. Solid (open) squares denote our (Cohen et al. 2000) redshifts. A second larger symbol denotes broad-line objects. Objects without redshifts are plotted at $z = -0.3$ (within a $6.5'$ radius) or at $z = -0.7$ (between $6.5'$ and $10'$).

of such high redshift AGN; Haiman & Loeb 1999.)

In Fig. 1 we show the redshift-magnitude relation for the galaxy population as squares (unidentified objects are plotted below $z = 0$ with different symbols). Broad-line sources (distinguished by a second larger symbol) are systematically the most optically luminous of the X-ray sources because of the AGN contribution to the light. Of the spectroscopic identifications, $> 80\%$ do not have broad optical or UV lines and $> 50\%$ show no obvious high ionization signatures of AGN activity.

All of the sources with $z > 1.6$ are either broad-line AGN or have narrow Ly α and/or CIII] 1909 Å emission. Intriguingly, while there are a substantial number of optically identified absorption-line sources with $z > 1.6$ known in the HDF-N and flanking fields, none are present in the X-ray sample.

In Fig. 2a we show histograms of the redshift distribution for $\Delta z = 0.1$ and $\Delta z = 0.01$ bins, and in Fig. 2b we show an R versus redshift blow-up of the two structures centered on $z = 0.843$ and $z = 1.0175$ (also detected in optical surveys; e.g., Cohen et al. 2000; Dawson et al. 2001) that are seen in the higher resolution histogram. These are the only two structures that contain at least 10 X-ray sources within 1000 km s^{-1} of the center positions. Fig. 2 suggests that there may be large scale structure in the field (spatially the sources also look clustered), but the structures do not dominate the number of X-ray sources in the sample so our overall redshift distribution should not be strongly affected by this cluster-

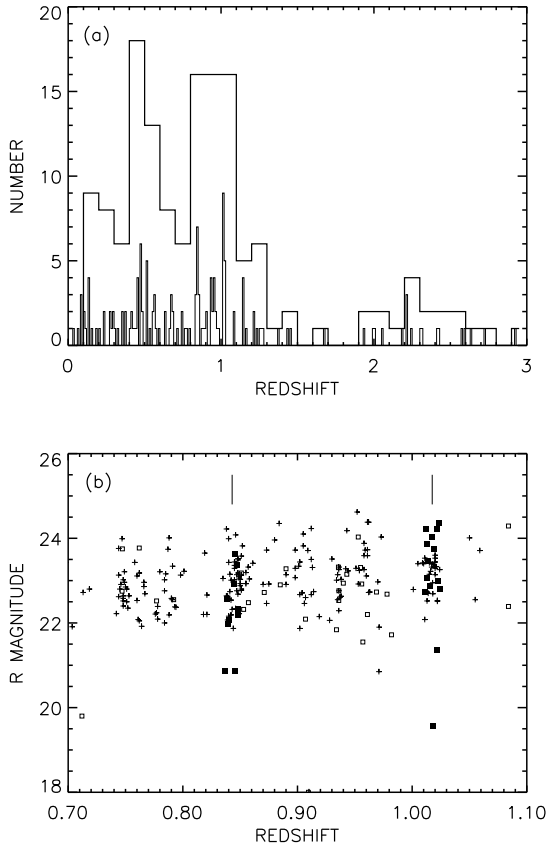


Fig. 2. (a) Redshift distribution for two bin sizes ($\Delta z = 0.1$ and $\Delta z = 0.01$). (b) R versus redshift blow-up shows the two structures centered at $z = 0.843$ and $z = 1.0175$. Sources within 1000 km s^{-1} of the center positions are denoted by solid squares, other X-ray sources by open squares, and field galaxies by plus signs.

ing. However, the number of sources in these structures (a total of 24 identified sources in the $z = 0.843$ and $z = 1.0175$ structures) is sufficiently large that it could account for a part of the field-to-field variation seen in the X-ray number counts (e.g., Cowie et al. 2002). Similar redshift structures have also been detected in the CDF-S exposure (Hasinger 2002).

3. SUPERMASSIVE BLACK HOLES

We can construct redshift slices of supermassive black hole growth from our *Chandra* data to learn about the evolutionary history of black holes. In Fig. 3 we show the redshift distribution versus 2–8 keV flux for two restricted uniform flux-limited subsamples: a ‘deep’ subsample (squares) from the 6.5’ radius region, and a ‘bright’ subsample (inverted triangles) from the 10’ radius region. In the deep (bright) subsample only sources detected in the 2–8 keV band above $5 \times 10^{-16} \text{ erg cm}^{-2} \text{ s}^{-1}$

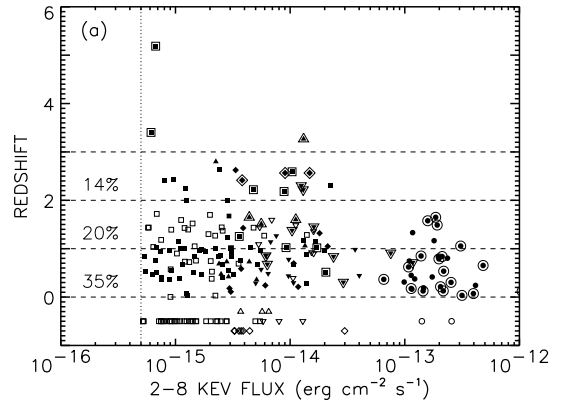


Fig. 3. Redshift versus 2–8 keV flux for the hard deep (squares) and bright (inverted triangles) subsamples. Broad-line sources are enclosed in a second larger symbol. Spectroscopically unidentified sources with (without) photometric redshifts are open symbols plotted at those redshifts (below the $z=0$ line). We also plot the Akiyama et al. (2000) data (circles) and the Barger et al. (2001a, b) SSA13 (diamonds) and A370 data (triangles). At the left is the percentage of the total light in the hard deep subsample that comes from spectroscopically identified point sources in each redshift interval.

($5 \times 10^{-15} \text{ erg cm}^{-2} \text{ s}^{-1}$) were considered. The *ASCA* Large Sky Survey data (circles) from Akiyama et al. (2000) and the SSA3 (diamonds) and A370 (triangles) data from Barger et al. (2001a, b) are also shown.

The percentage of the total light in the deep subsample that comes from spectroscopically identified point sources in each redshift interval is indicated. At least 35% arises below $z = 1$ and at least 55% arises below $z = 2$. These percentages increase to 40% and 73% if we include the sources with photometric redshifts. Although not shown, similar results are obtained for the soft deep subsample. Thus, the bulk of the total 2–8 keV and 0.5–2 keV flux in the deep subsamples arises at recent times, and black hole growth is *not* only associated with the galaxy formation era.

4. HIGH ENERGY XRB CONTRIBUTIONS

A simple model which assumes a fixed intrinsic photon index modified at low energies by photoelectric absorption from a varying intrinsic column density describes the (0.5–2 keV)/(4–8 keV) versus (2–4 keV)/(4–8 keV) counts ratios reasonably well with an intrinsic Γ between 1.5 and 2.5. From the (0.5–2 keV)/(2–8 keV) counts ratio we find that the broad-line sources have an extremely narrow hardness range which would correspond to a spectral in-

dex of $\Gamma = 1.7$ in the absence of optical depth effects. Nearly all the sources have $\Gamma < 1.8$. For a $\Gamma = 1.8$ input spectrum and absorption by the photoelectric cross-section, we infer intrinsic N_H values that range from about 10^{21} cm^{-2} to $5 \times 10^{23} \text{ cm}^{-2}$; only a small number of spectroscopically unidentified sources potentially could have higher column densities. Our description is simple, so we caution that there could still be some Compton-thick sources in our sample, even if we do not recognize them as such. It is therefore interesting to consider whether the XRB *requires* contributions from a population of Compton-thick sources.

In Fig. 4 we plot the total XRB contributions from the 2–8 keV deep subsample (thick solid line) computed assuming an intrinsic $\Gamma = 1.8$ power-law for each source, together with an optical depth for each source determined from the (0.5–2 keV)/(2–8 keV) counts ratio. The deep subsample produces about 87% of the *HEAO-A* background at 3 keV and 57% at 20 keV. However, when the *Chandra* data are normalized at 3 keV to the higher *ASCA* or *BeppoSAX* measurements, then the shape from the *Chandra* sources matches fairly well that of the observed XRB (thin solid line) at both energies. Thus, whether the match to the high energy XRB requires either a substantial population of as-yet undetected Compton-thick sources or some change in the intrinsic spectral shape of the current sources from the simple power-law dependence clearly depends critically on how the low energy and high energy XRB measurements tie together.

REFERENCES

Akiyama, M., et al. 2000, *ApJ*, 532, 700
 Barden, S. C., Armandroff, T., Muller, G., Rudeen, A. C., Lewis, J., & Groves, L. 1994, *Instrumentation in Astronomy VIII*, ed. D.L. Crawford and E.R. Craine, SPIE Vol. 2198, p. 87
 Barger, A. J., Cowie, L. L., Mushotzky, R. F., & Richards, E. A. 2001a, *AJ*, 121, 662
 Barger, A. J., et al. 2001b, *AJ*, 122, 2177
 Boldt, E. 1987, *Phys. Rep.*, 146, 215
 Brandt, W. N., et al. 2001, *AJ*, 122, 2810
 Campana, S., Moretti, A., Lazzati, D., & Tagliaferri, G. 2001, *ApJ*, 560, L19
 Cohen, J. G., et al. 2000, *ApJ*, 538, 29
 Cowie, L. L., et al. 2001, *ApJ*, 551, L9
 Cowie, L. L., et al. 2002, *ApJ*, 566, L5
 Crawford, C. S., Fabian, A. C., Gandhi, P., Wilman, R. J., & Johnstone, R. M. 2001, *MNRAS*, 324, 427

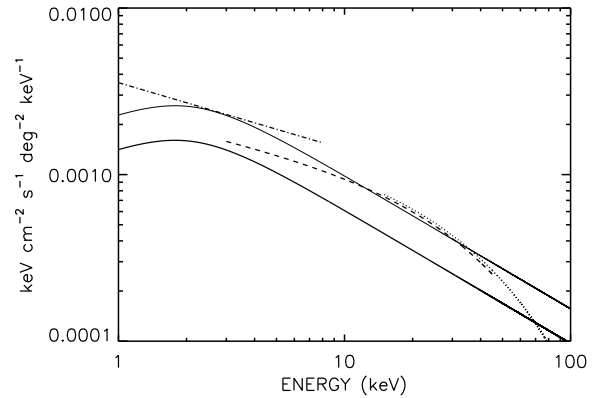


Fig. 4. Total XRB contribution from the 2–8 keV deep subsample (thick solid line) based on an intrinsic $\Gamma = 1.8$ power-law dependence combined with an opacity determined from the (0.5–2 keV)/(2–8 keV) counts ratio for each source in the subsample. Dashed (dotted) line is the *HEAO-A* XRB measurement from Boldt 1987 (Gruber et al. 1984; Gruber 1992; Fabian & Barcons 1992). Dot-dashed line is the *BeppoSAX* measurement of Vecchi et al. (1999). Other measurements in the 1–10 keV range lie between the *HEAO-A* and *BeppoSAX* measurements. Thin solid line is the total XRB contribution from the 2–8 keV deep subsample, renormalized to match the *BeppoSAX* measurement at 3 keV.

Dawson, S., Stern, D., Bunker, A., Spinrad, H., & Dey, A. 2001, *AJ*, 122, 598
 Fabian, A. C. & Barcons, X. 1992, *ARA&A*, 30, 429
 Fabian, A. C. & Iwasawa, K. 1999, *MNRAS*, 303, L34
 Giacconi, R., et al. 2002, *ApJS*, 139, 369
 Gruber, D. E., Rothschild, R. E., Matteson, J. L., & Kinzer, R. L. 1984, *Max Planck Inst. Rep.*, 184, 129
 Gruber, D. E. 1992, in *The X-ray Background*, ed. X. Barcons & A. C. Fabian, (Cambridge: Cambridge Univ. Press), p. 44
 Haiman, Z. & Loeb, A. 1999, *ApJ*, 521, L9
 Hasinger, G. 2002, in *New Visions of the X-ray Universe in the XMM-Newton and Chandra Era*, ed. F. Jansen, in press (*astro-ph/0202430*)
 Miyazaki, S., Sekiguchi, M., Imi, K., Okada, N., Nakata, F., & Komiyama, Y. 1998, in *Proc. SPIE Vol. 3355, Optical Astronomical Instrumentation*, ed. S. D’Odorico, p. 363
 Oke, J.B., et al. 1995, *PASP*, 107, 375
 Rosati, P., et al. 2002, *ApJ*, 566, 667
 Vecchi, A., Molendi, S., Guainazzi, M., Fiore, F., & Parmar, A.N. 1999, *A&A*, 349, L73

A.J. Barger: Department of Astronomy, University of Wisconsin, 475 N. Charter St., Madison, WI, 53705, USA (barger@astro.wisc.edu).